

AD-AU90 442

ARMY ARMAMENT RESEARCH AND DEVELOPMENT COMMAND ABERD--ETC F/G 19/1
RECENT RESEARCH ON PHOSPHORUS SMOKE, (U)
JUN 80 E W STUEBING, R H FRICKEL, G O RUBEL

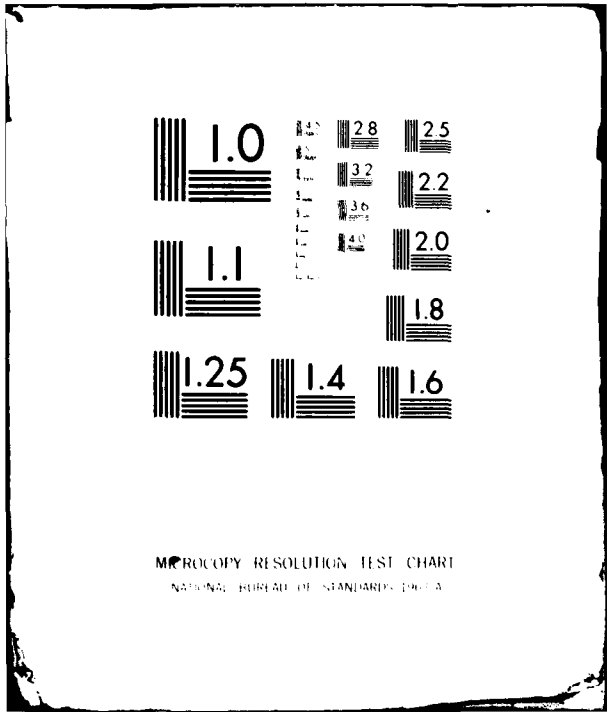
UNCLASSIFIED

NL

1 of 1
AD
A90417



END
DATE
FILMED
11 80
DTIC



MICROCOPY RESOLUTION TEST CHART
NATIONAL BUREAU OF STANDARDS-1963-A

*STUEBING, FRICKEL, & RUBEL

OCT 20 1980

AD A 090442

12 / 15

LEVEL

S

A

6

RECENT RESEARCH ON PHOSPHORUS SMOKE (1)

10 EDWARD W. STUEBING, Ph.D.
ROBERT H. FRICKEL
GLENN O. RUBEL

CHEMICAL SYSTEMS LABORATORY, USAARRADCOM
ABERDEEN PROVING GROUND, MD 21010

11

I. INTRODUCTION

The optical extinction coefficients of phosphorus smokes in various regions of the spectrum are expected to depend on relative humidity due to the hygroscopic nature of the aerosol. They also depend on the amount of smoke (C- & Product) present. These are important problems for systems analysts who model the effectiveness of smoke munitions, and for scientists conducting field tests on smokes who measure the transmission through smoke clouds and use assumed extinction coefficients to calculate the amount of smoke present from Beer's law. The growth of smoke particles with increasing relative humidity changes their size distribution and their refractive indices, both of which alter the extinction cross sections (m^2 /particle). In addition, the density of droplet material changes which causes further variation in the aerosol extinction coefficient (m^2 /gram). This paper presents the results of a study of the dependence of visible, mid-IR, and far-IR extinction coefficients on relative humidity and includes consideration of non-Beer's law behavior of these extinction coefficients with (concentration) x (pathlength) product. The model used for relative humidity dependence assumes that the aerosol is composed of phosphoric acid for optical (refractive index) properties. The adequacy of this assumption is examined by comparison with experimental data on phosphorus smokes. The examination of deviations from Beer's law is based on actual phosphorus smoke extinction data and results in extinction coefficients for use in mid and far IR regions which should be satisfactory at relative humidities below 70%.

II. RELATIVE HUMIDITY CONTROLLED GROWTH OF PHOSPHORUS SMOKE

DDC FILE COPY

This document has been approved for public release and sale; its distribution is unlimited.

293

410170 2/180 10 17 020

A model for the growth of phosphoric acid droplets due to dilution by condensation of water vapor as relative humidity increases has been developed by Rubel⁽¹⁾, and its implications for relative humidity dependence of the optical properties of phosphoric acid aerosols have been examined by Frickel, et. al.⁽²⁾. The application of the results to phosphorus smoke is questionable because there exists conclusive evidence⁽³⁾ that phosphorus smoke particles are not composed of pure phosphoric acid, and because the description used for the water vapor pressure over phosphoric acid solution was accurate for the relative humidity range 0.10-0.90, whereas the principle growth effects occurred at relative humidities above 0.90. Rubel has recently completed a new droplet growth model⁽⁴⁾ which incorporates a modified description of droplet water vapor pressure (water activity) accurate to relative humidities of 0.99, and has treated the acid concentration as an unspecified mixture of acids (e.g. pyrophosphoric, metaphosphoric, and orthophosphoric acids) characterized by an association parameter, a , which reduces the concentration of solute ions available compared to a solution of orthophosphoric acid having the same acid weight fraction. By comparison to various experimental data Rubel⁽⁴⁾ has found that values of a between 1.3 and 1.5 seem appropriate to phosphorus smoke particles. The value $a=1.5$ is used here because it represents the greatest variation from the previous⁽²⁾ pure orthophosphoric acid ($a = 1.0$) model and therefore provides a "worst case" test of the errors in the simpler model of reference⁽²⁾.

An analysis of the kinetics of the particle growth process⁽⁴⁾ shows that for relative humidities below 95% the particles very rapidly reach equilibrium with their environment so that these results would be expected to apply to a real smoke in the open atmosphere. This model predicts that all particles in a polydispersion change size by a common factor when relative humidity changes. Consequently, if a log-normal aerosol size distribution characterized by a mass median diameter (MMD) and geometric standard deviation (σ_g) is subjected to a change in relative humidity, the new size distribution will remain log-normal and will have the same σ_g ; however, the MMD will be shifted according to the common size change factor. In particular, the radius (r) of a particle at any relative humidity (Ψ) can be predicted from its size at $\Psi = 0$ (denoted r_0). This size shift is given by

$$r = f^{1/3}(\Psi) r_0 \quad (1)$$

where

$$f(\Psi) = \frac{a\rho_1 M_2 + x(M_1\rho_2 - a\rho_1 M_2)}{a\rho_1 M_2(1-x)} \quad (2)$$

294

*STUEBING, FRICKEL, & RUBEL

with

$$x = \begin{cases} \frac{2.152 - (0.655 - 0.632\Psi)^{\frac{1}{2}}}{2} & 0.75 \leq \Psi \leq 0.995 \\ 0.632 \cdot \cos \left[\frac{\cos^{-1} (1.175 - 1.928\Psi)}{3} + 240 \right] + 0.803 & 0.10 \leq \Psi \leq 0.75 \end{cases} \quad (3)$$

(degrees)

where ρ is density, M is molecular weight, and the subscripts are 1 for water and 2 for H_3PO_4 : $M_1=18$; $M_2=98$, $\rho_1=1.0$, $\rho_2=1.87$. The parameter a describes the average degree of combination of the phosphate moiety in the acid mixture: $a=1$ corresponds to pure orthophosphoric acid, $a=4$ would apply to pure tetrametaphosphoric acid⁽⁴⁾. For this study the value $a=1.5$ was used as discussed above. The dilution of the drop with increasing relative humidity is given by

$$F = \frac{\rho_1 \rho_2 [M_1 x + a M_2 (1-x)]}{a \rho_1 M_2 + x (M_1 \rho_2 - a M_2 \rho_1)} \quad (4)$$

where F is the weight fraction of acid in the drop. For calculations involving density of the smoke droplets, tabulated values⁽⁵⁾ of the specific gravity of aqueous phosphoric acid solutions corresponding to acid weight fraction given by equation (4) were used, see Table I.

TABLE I. ACID CONCENTRATIONS WITH THEIR CORRESPONDING RELATIVE HUMIDITIES FOR $a=1.5$, AND SOLUTION DENSITY.

Weight Fraction Acid	Relative Humidity ($a=1.5$)	Density (ρ/cc)
0.05	1.00	1.025
0.10	0.99	1.053
0.20	0.97	1.112
0.40	0.90	1.254
0.50	0.82	1.335
0.65	0.64	1.475
0.75	0.44	1.579
0.95	0.16	1.629

Experiments have shown that log-normal distributions provide reasonable descriptions for phosphorus smokes. Therefore, once a size

275

*STUEBING, FRICKEL, & RUBEL

distribution is established for pure acid drops* produced by the smoke munition, called hereafter the "primitive acid nucleus" distribution, then the actual aerosol size distribution achieved at relative humidity Ψ will be given by

$$\frac{dM}{M d \ln(d)} (2\pi \ln(\sigma_g))^{-\frac{1}{2}} \exp\left\{-\left[\ln(d) - \ln(f^{1/3}(\Psi)d_0)\right]^2 / 2 \ln^2 \sigma_g\right\} \quad (5)$$

where M is the mass distribution function, d_0 is the mass median diameter of the distribution of primitive acid nuclei and σ_g is the geometric standard deviation of the distribution of primitive acid nuclei (and also of all distributions derived from it by hydration). The size distribution of smokes at various relative humidities then can be predicted provided d_0 and σ_g are determined from data taken at a time when significant distribution disturbing processes (e.g. coagulation, sedimentation) are absent.

III. SIZE DISTRIBUTION OF PRIMITIVE ACID NUCLEI PRODUCED BY PHOSPHORUS MUNITIONS

Given size distribution data (d , σ_g) on any phosphorus smoke cloud and the relative humidity at which it was determined, equations (1)-(5) can be used to extrapolate back to the primitive acid nucleus distribution for that cloud. If all phosphorus-based munitions produced identical smokes, then all such extrapolations would produce the same parameters d_0 and σ_g . A number of experimental measurements made on a variety of white phosphorus and red phosphorus munitions⁽⁶⁾ are shown in Table II along with the extrapolated primitive acid nucleus distribution from each for $a = 1.5$.

The particle size measurements were made using an Anderson Impactor, and relative humidity was determined either by dew point hygrometer or gravimetric determination of water vapor collected on magnesium perchlorate. The data was selected from chamber experiments which met the following three conditions:

(1) Smoke concentrations were relatively low ($<1.0 \text{ gm/m}^3$) to help insure that size distributions would not be pushed toward larger sizes by coagulation effects in smokes denser than expected in the field.

*These are conceptually the drops that would be formed if there was just enough water in the atmosphere to react chemically with the P_2O_5 to produce H_3PO_4 but no additional water for hydration or dilution. These drops probably do not exist physically; they merely provide a mathematical basis for calculating the size changes of true size distributions at relative humidities in the range of 10-99.5%.

276

TABLE II. EXPERIMENTALLY MEASURED PARTICLE SIZE DISTRIBUTIONS FOR PHOSPHORUS SMOKES AND THEIR PRIMITIVE ACID NUCLEUS DISTRIBUTIONS

Case	EXPERIMENTAL DATA			Acid Nucleus* MMD(μ m)=1.5
	MMD(μ m)	σ_g	Relative Humidity	
1	0.72	1.44	0.37	0.62
2	0.69	1.48	0.23	0.62
3	0.69	1.40	0.16	0.63
4	0.75	1.44	0.34	0.65
5	0.77	1.47	0.12	0.71
6	0.86	1.51	0.51	0.71
7	0.87	1.43	0.22	0.79
8	0.91	1.46	0.20	0.82
9	0.93	1.44	0.17	0.85
10	1.02	1.45	0.19	0.92

*See text. The acid nucleus distribution has the same σ_g as the experimental data.

(2) The σ_g was in the vicinity of 1.4, a value known theoretically (7) to typify a "mature" log-normal distribution (in the sense that coagulation processes carry any log-normal distribution of $\sigma_g \neq 1.4$ toward a distribution with $\sigma_g = 1.4$).

(3) The relative humidity was not established artificially in the chamber by introducing water vapor. Therefore, the humidity in the laboratory matched closely that within the chamber for the selected experiments so there is no problem with size distribution data being distorted due to any sample changes on being removed for gravimetric analysis from a cloud of one humidity into a laboratory at a different humidity.

The results tabulated in Table II suggest that a σ_g slightly higher than 1.4 typifies phosphorus smokes; therefore, the value $\sigma_g = 1.45$ was selected for this study. Because the mass median diameters for the primitive acid nucleus distributions appear to vary too widely to accept a single number as typical of phosphorus smoke, calculations were performed for three values: $d_0 = 0.60, 0.75, 0.90$.

IV. REFRACTIVE INDICES FOR PHOSPHORIC ACID

Refractive indices for phosphoric acid in the 3-5.5 μ m and 7-12 μ m regions of the infrared have been measured for a number of acid concentrations (8). These were used for Mie calculations in which at each relative humidity the acid concentration of the drop is given by equation (4) and the size distribution by equation (9). The refractive

297

*STUEBING, FRICKEL & RUBEL

index in the visible was taken to be constant with respect to wavelength, and its variation with acid concentration was estimated from⁽⁹⁾.

$$n = 1.333977 + 0.001999 w^{1/2} + 0.07155w + 0.0868841 w^{3/2} - 0.2375104 w^2 + 0.3625678 w^{5/2} - 0.1669960 w^3 \quad (6)$$

where w is the weight fraction concentration of H_3PO_4 over the range $0 < w < 0.90$.

V. LIMITATIONS OF THE PHOSPHORUS SMOKE MODEL

Inaccuracies due to errors in the size distribution derived from Table II and in the visible refractive index from equation (6) have been examined by parametric calculations. The size distribution was varied over the full range of MMD's observed in Table II in the course of our calculations. It has a significant effect on the extinction coefficient and is therefore shown explicitly in the results section as an inherent range of variation in the extinction by phosphorus smoke. Exploratory calculations on the effects of varying σ_g were performed. The resulting variation in extinction is somewhat less significant than the MMD variation; hence the variation plotted in our results is a reasonable estimate of optical variation due to MMD and σ_g variation. The real part of the visible refractive index was varied about the value given in equation (6), which applies at the wavelength $0.546 \mu m$, by a proportion similar to the variation with respect to wavelength in the visible of the refractive index of water. In addition, the effects of adding a complex component up to 10^4 times that of water was examined. The range of resulting uncertainty in the properties of phosphorus smoke was less than $\pm 1.0\%$. However, there remains a more fundamental limitation on the application of the model used here to phosphorus smokes. It is known⁽³⁾ that during the period of tactical significance (say, 20 minutes after generation) that phosphorus smoke is not composed of phosphoric acid. The model used here relies on phosphoric acid data (e.g., H_2O vapor pressure vs solution concentration adjusted for combination of phosphates in the pyro and meta components of the mixture) for the growth properties of droplets and for the optical properties (refractive indices). The growth model has not yet been tested against phosphorus smoke, although such studies are presently underway⁽⁴⁾. For this study, sensitivity to errors in the growth model is reduced by using the same equations to extrapolate back to the primitive acid nucleus distribution from actual phosphorus smoke size distribution data as are used in running the distribution forward with increasing humidity, and by considering a fairly wide range of primitive size distributions. The optical model

*STUEBING, FRICKEL & RUBEL

has been examined in the infrared⁽³⁾; it gives a reasonably accurate spectral curve in the 3-5.5 μm region, but is quite inadequate in the 7-12 μm region. Therefore, predicting the relative-humidity dependent phosphorus smoke extinction at individual wavelengths from this study would be perilous, particularly in the 7-12 μm region. Integrating over wavelength to produce an overall extinction coefficient for the region may produce a somewhat closer representation of the behavior of phosphorus smoke; however, it is probably better to pay more attention to the predicted trend in 7-12 μm extinction with relative humidity than to its absolute value. As an aid to making an empirical adjustment by scaling the phosphoric acid extinction to the level of phosphorus smoke extinction, the results of this model have been compared with measurements made on phosphorus smoke at low relative humidities. This comparison is discussed in Section 8.

VI. DEFINITION OF OVERALL EXTINCTION COEFFICIENTS FOR THE VISIBLE, MID-IR, AND FAR-IR

The problem of defining an overall extinction coefficient for a smoke in each spectral region has been previously discussed with respect to deviations from Beer's law⁽¹⁰⁾. The results showed that effective extinction coefficients in a wavelength region $\Delta\lambda$, $\alpha_{\text{eff}}(\Delta\lambda)$, were often dependent on the (concentration) x (pathlength) product. This is especially true for phosphorus smokes in the 7-12 μm region.

The calculations used here follow those of reference⁽¹⁰⁾; they have been extended to include the visible region. The measurement of light transmission (T) through a smoke cloud is often used in field experiments to infer the amount (C \cdot l product) of the smoke in the optical path. This inference is made using Beer's law:

$$T(\lambda) = \frac{I(\lambda)}{I_0(\lambda)} = e^{-\alpha(\lambda)C\ell} \quad (7)$$

where $I_0(\lambda)$ = the light intensity at wavelength λ measured by the detector with no smoke in the path.

$I(\lambda)$ = the light intensity at wavelength λ measured by the detector with smoke in the path.

$\alpha(\lambda)$ = the extinction coefficient (commonly m^2/gm) at wavelength λ .

C = concentration (commonly gm/m^3).

ℓ = path length (commonly m).

*STUEBING, FRICKEL & RUBEL

The inference is generally valid provided the measurement is made at a single wavelength (e.g. a laser transmissometer) and the value of α is known for that wavelength, or if the transmission measurement is made over a wavelength band ($\Delta\lambda$) provided that $\alpha(\lambda)$ is constant over the region $\Delta\lambda$. These conditions are usually well satisfied in the narrow band pass of a spectrophotometer. However, in some field measurements, broadband radiometers (e.g. 3-5.5 μm or 7-12 μm) are used for the transmission measurement. Beer's law does not generally apply in these cases with a single effective α (e.g. α_{eff} (7-12 μm)). Should one attempt to define such an effective α from the equation

$$T(\Delta\lambda) = e^{-\alpha_{\text{eff}}(\Delta\lambda) C\ell} \quad (8)$$

by measuring T under conditions of known $C\ell$ and solving for $\alpha_{\text{eff}}(\Delta\lambda)$, different values of $\alpha_{\text{eff}}(\Delta\lambda)$ would be found for different values of $C\ell$. This effect is most prominent in cases where $\alpha(\lambda)$ varies strongly over the region $\Delta\lambda$, and disappears as $\alpha(\lambda)$ becomes constant over the region $\Delta\lambda$.

The treatment of broadband transmission behavior in the infrared may be made analogously to the photometric treatment of broadband transmission in the visible with the following definitions: luminance, $L(\Delta\lambda)$, is the apparent brightness of the target; transmittance, $Tr(\Delta\lambda)$, is the ratio of luminance with smoke in the path to luminance without smoke and corresponds to the transmission in Beer's law. The governing equation is then:

$$Tr(\Delta\lambda) = \frac{L(\Delta\lambda)}{L_o(\Delta\lambda)} = \frac{\int_{\lambda_1}^{\lambda_2} S(\lambda) e^{-\alpha(\lambda)C\ell} D(\lambda) d\lambda}{\int_{\lambda_1}^{\lambda_2} S(\lambda) D(\lambda) d\lambda} \quad (9)$$

where $S(\lambda)$ = source signature as a function of wavelength.

$D(\lambda)$ = the detector response curve as function of wavelength.

The denominator of equation (9), $L_o(\Delta\lambda)$, gives the original apparent brightness of the source as seen by the detector; the numerator, $L(\Delta\lambda)$, gives the reduced apparent brightness when a smoke characterized by $\alpha(\lambda)$, C , and ℓ intervenes. For the purpose of calculating $Tr(\Delta\lambda)$, it is only necessary to have relative curves for the source and detector.

The source functions, $S(\lambda)$, in the 3-5.5 and 7-12 μm regions are taken to be 300°K blackbodies⁽¹⁰⁾; the visible source is the standard CIE-C (artificial daylight) function⁽¹¹⁾. The detector response functions, $D(\lambda)$, in the 3-5.5 and 7-12 μm regions are those of typical

300

*STUEBING, FRICKEL & HOLST

InSb and HgCdTe detectors⁽¹⁰⁾; the visible detector is the standard photopic observer⁽¹¹⁾.

VII. RESULTS

The particle growth model is shown in Figure 1 where the growth curves of the mass median diameters of each of the three primitive nuclei distributions is given. The acid concentrations for which refractive index data were available; and their corresponding relative humidities are shown in Table I. The computed extinction coefficients are unchanged from those previously reported⁽²⁾; however they are associated with changed values of relative humidity because the mixed-acids model requires somewhat higher relative humidities than does pure phosphoric acid in order to produce the same degree of droplet dilution, c.f. Table I.

Integrated extinction coefficients will depend on $C \cdot l$ product as well as relative humidity. For the visible and mid-IR, the $C \cdot l$ dependence is weak. In only a very few of the cases examined did the reduction in α_{eff} exceed 2% over the range $0.1 < C \cdot l < 20$. In the visible and mid-IR, the variation in α_{eff} due to uncertainty in the primitive acid nucleus size distribution far outweighs effects due to $C \cdot l$. However, in the far-IR there is a significant decrease in α_{eff} (7-12) with increasing $C \cdot l$ product at low and moderate relative humidities, which is significant in comparison with the effect of the uncertain size distributions. This is shown for three relative humidities in Figure 2.

Because of the Beer's law deviation problem with integrated extinction coefficients, in order to examine the effect of relative humidity on integrated extinction coefficients it is necessary to choose a value of $C \cdot l$ product. From the above discussion, it makes little difference in the visible and mid-IR which $C \cdot l$ is used. Therefore, the $C \cdot l$ for this study was selected to be one of interest to measurements in the far-IR. From Figure 2, the values of the $C \cdot l$ dependent α_{eff} 's are in the range 0.25-0.30; therefore a $C \cdot l = 5.0$ was chosen as this provides sufficient smoke to reduce transmission in the far-IR to 20-30%. The results for each spectral region are shown in Figures 3-5. The extinction coefficients in these figures are in the conventional units of m^2 per gram of aerosol material suspended. It is also of interest to examine the extinction coefficient in terms of mass of elemental phosphorus delivered by the munition and its dependence on relative humidity, Figures 6-8. These data are of value to systems analysts modeling smoke effects as they include the humidity dependence of the "yield factor". It can be seen from Figures 3-8 that although the extinction coefficient per unit mass of smoke

301

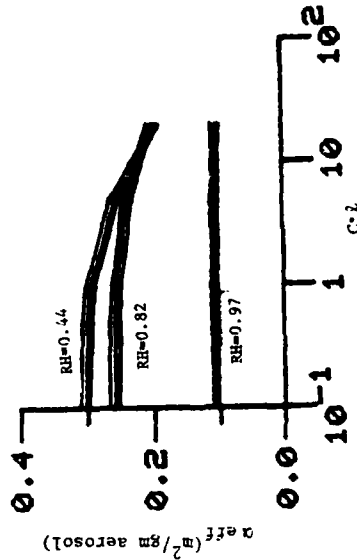


Figure 2. Variation of Far-IR Extinction Coefficient with C-1 Product for Phosphoric Acid Aerosol. At each relative humidity the region between the lines represents the expected range of variation due to particle size variations typical of phosphorus smokes (see text).

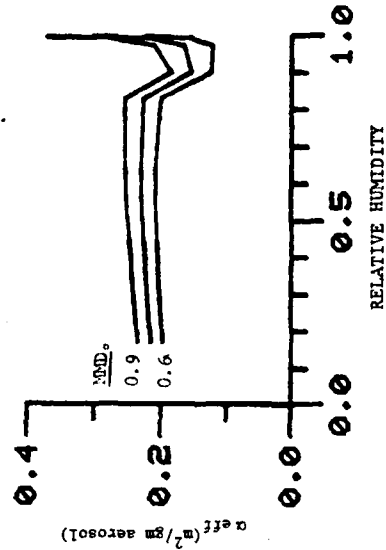


Figure 4. Mid-IR Extinction Coefficient for Phosphoric Acid Aerosol. The region between the lines represents the expected range of variation due to particle size variations typical of phosphorus smokes (see text).

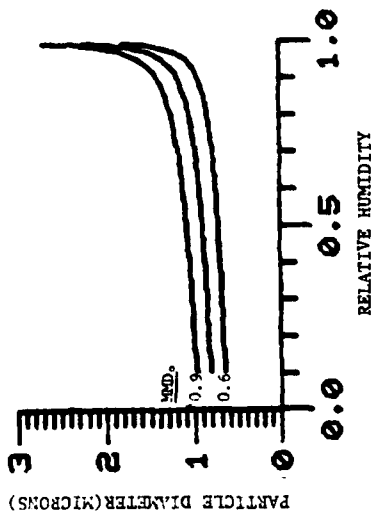


Figure 1. Growth of Mass Median Diameter (MDD) with Increasing Relative Humidity for Primitive Acid Nuclei Distributions Having Initial MDD's (MDD₀) of 0.6, 0.75, and 0.90, using association parameter $\alpha = 1.5$.

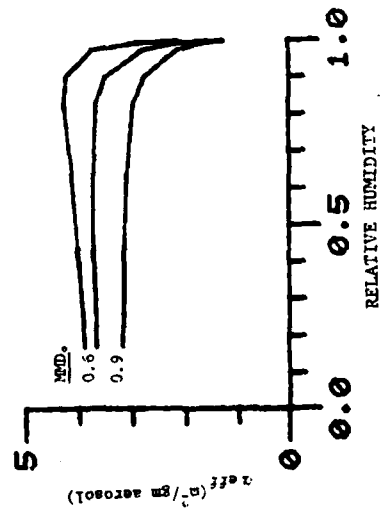


Figure 3. Visible Extinction Coefficient for Phosphoric Acid Aerosol. The region between the lines represents the expected range of variation due to particle size variations typical of phosphorus smokes (see text).

302

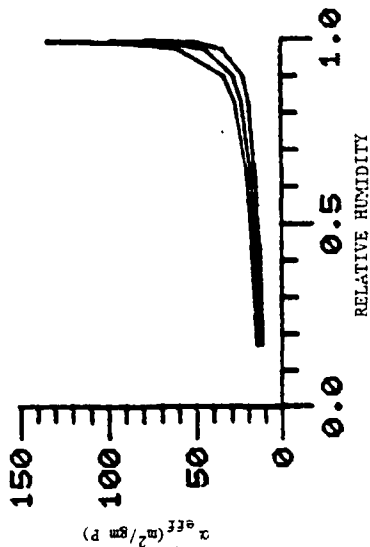


Figure 6. Visible Extinction Referred to Mass of Phosphorus in the Aerosol (c.f. fig. 3).

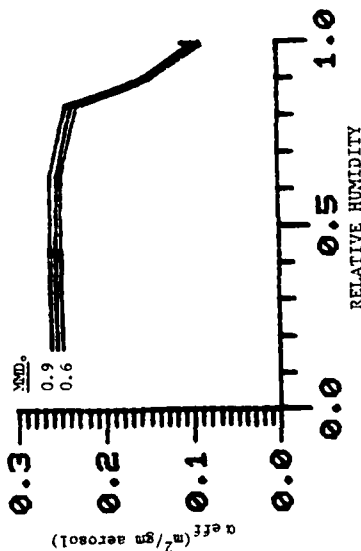


Figure 5. Far-IR Extinction Coefficient for Phosphoric Acid Aerosol. The region between the lines represents the expected range of variation due to particle size variations typical of phosphorus smokes (see text).

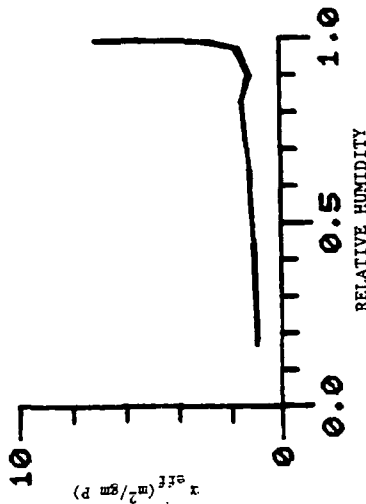


Figure 8. Far-IR Extinction Referred to Mass of Phosphorus in the Smoke (c.f. figure 5).

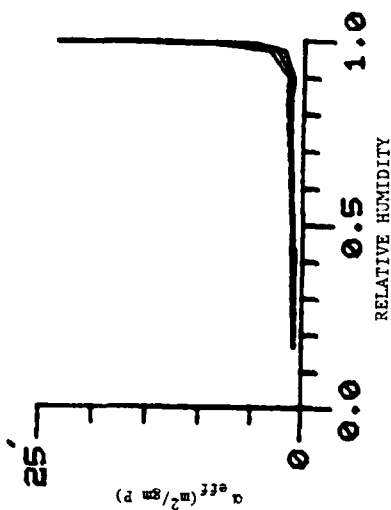


Figure 7. Mid-IR Extinction Referred to Mass of Phosphorus in the Aerosol (c.f. figure 4).

303

*STUEBING, FRICKEL, & RUBEL

decreases with dilution (at about 80% relative humidity) the increase of mass due to extraction of water from the atmosphere tends to compensate for this, so that extinction per unit mass of airborne phosphorus is relatively constant over most of the relative humidity range, and increases dramatically for relative humidity greater than 0.9.

VIII. COMPARISON WITH PHOSPHORUS SMOKE DATA

Integrated extinction coefficients in the mid-IR and far-IR have been computed from actual phosphorus smoke spectra⁽¹⁰⁾. The spectral data used was averaged over several experiments conducted at different relative humidities, all of which were below 70%. The present model predicts little change in extinction coefficient for relative humidities between 10 and 70%; therefore, it is reasonable to use an α_{eff} computed from spectra averaged over several relative humidities in this range for comparison purposes. In the mid-IR the phosphorus smoke data⁽¹⁰⁾ give $\alpha_{\text{eff}}=0.25$, which is at the very top of the range predicted by the present model in Figure 4. In the far-IR the phosphorus smoke data⁽¹⁰⁾ gives $\alpha_{\text{eff}}=0.32$ for the $C \cdot \ell$ product value 5.0 used in Figure 5, which is approximately 20% higher than the value given by the phosphoric acid optical model.

Systems analysts modeling smoke effects and scientists conducting smoke field tests need working values for integrated extinction coefficients for phosphorus smoke. The results so far suggest that Beer's law deviations are relatively important only in the far IR (7-12 μm) region, and then only at low and moderate relative humidities, c.f. Figure 2; over most of this range, relative humidity has little effect, c.f. Figure 5. The experimental spectra of phosphorus smokes for relative humidities below 70% have been used to examine the $C \cdot \ell$ dependence of the far infrared extinction coefficient⁽¹⁰⁾. Data on smokes produced by both white phosphorus and red phosphorus have been examined and are very nearly identical. Both may be treated by the results given here, which are shown in Figure 9. If this change in broadband extinction coefficient with $C \cdot \ell$ product is ignored for phosphorus smokes in the 7-12 μm window, quite serious errors could occur. For example, with measured transmittance of 5% and the low $C \cdot \ell$ limit of $\alpha(\lambda)=0.37$ chosen as $\alpha_{\text{eff}}(\Delta\lambda)$, the $C \cdot \ell$ calculated in a field experiment is in error by 30%.

In order to provide a means for correcting for these errors, equation (9) has been used to calculate the transmittance expected from various $C \cdot \ell$ values and the results tabulated in Table III. The tables cover transmittance down to 0.1% as the lower limit likely to be achieved by a broadband transmissometer. The table can be entered

36-1

*STUEBING, FRICKEL, & RUBEL

TABLE III. TRANSMITTANCE, C·L (gm/m²), AND ALPHA (m²/gm) VALUES FOR PHOSPHORUS SMOKE AGAINST A 100°K BLACKBODY TARGET IN THE 7-12 μm WINDOW

Trans	C·L	Alpha	Trans	C·L	Alpha	Trans	C·L	Alpha
0.964	0.1	0.37	0.123	7.0	0.30	0.308	12.0	0.22
0.829	1.2	0.37	0.398	8.0	0.29	0.397	13.0	0.22
0.696	0.3	0.37	0.678	9.0	0.28	0.306	14.0	0.21
0.564	1.4	0.37	1.064	10.0	0.28	0.305	15.0	0.21
0.434	0.5	0.36	0.352	11.0	0.27	0.305	16.0	0.21
0.304	0.6	0.36	0.043	12.0	0.26	0.304	17.0	0.21
0.176	0.7	0.26	0.036	13.0	0.26	0.003	18.0	0.20
0.749	0.8	0.26	0.030	14.0	0.25	0.303	19.0	0.20
0.723	0.9	0.26	0.025	15.0	0.24	0.003	20.0	0.20
0.998	1.0	0.26	0.021	16.0	0.24	0.002	21.0	0.20
0.438	1.1	0.25	0.018	17.0	0.24	0.002	22.0	0.20
0.362	1.2	0.24	0.015	18.0	0.23	0.002	23.0	0.19
0.269	4.0	0.23	0.013	19.0	0.23	0.001	24.0	0.19
0.204	5.0	0.22	0.011	20.0	0.22	0.001	25.0	0.19
0.157	6.0	0.21	0.010	21.0	0.21	0.001	26.0	0.19

TABLE IV. EFFECTIVE EXTINCTION COEFFICIENTS FOR PHOSPHORUS SMOKE

Window Region	α _{eff}	Applicable Range	
		C·L (gm/m ²)	Transmittance in Window
7-12	0.25	0-30	0.901 - 1.0
7-12	0.35	3-2	0.5 - 1.0
	0.32	2-8	0.1 - 0.5
	0.25	8-20	0.01 - 0.1

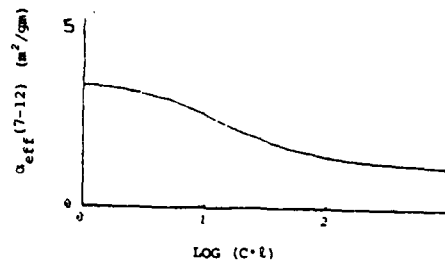


Figure 9. Variation in Effective Extinction Coefficient with C·L Product in the Far-IR for Phosphorus Smoke.

with the observed transmittance and the corresponding C·L product read out. The numerical values of the "effective α's" are also tabulated. Although the detector response curves are quite generally typical, as are the smoke extinction curves, the source curves used in generating these tables are for a 300°K blackbody. In some experiments sources of quite different spectral characteristics are employed, in which cases these calculations should be repeated.

IX. CONCLUSIONS

1. A model for the expected range of particle size distribution expected in phosphorus smokes and their variation with relative humidity has been proposed: Figure 1.
2. Using these size distributions and optical constants for appropriate dilutions of phosphoric acid, estimates of the integrated extinction coefficients in the visible, mid-IR, and far-IR were computed as functions of relative humidity: Figures 3-5.
3. These estimates were tested against a small amount of phosphorus smoke data in the mid- and far-IR. They appear reasonably close in the mid-IR and low by 20-25% in the far-IR where phosphoric acid optical constants are known to poorly represent phosphorus smoke⁽³⁾. The smoke data used for comparison did not address variation with relative humidity.
4. The model predicts trends in α_{eff} with relative humidity in each

305

*STUEBING, FRICKEL, & RUBEL

spectral region. The extinction coefficients remain relatively constant in each region for relative humidities below 70%. The trends above 70% in each region could serve in the design of experiments on phosphorus smokes. The trends in extinction coefficients shown in Figures 3-5 all indicate a decrease above 80% relative humidity; it should be kept in mind that the suspended mass of the particles increases due to extraction of additional water from the atmosphere so that any given cloud does not become significantly less opaque with increasing relative humidity and increases greatly in opacity at humidities above 90%, as shown in Figures 6-8.

5. Although Beer's law does not apply generally for broadband extinction effects, it is often a reasonably good approximation. In such cases an effective extinction coefficient, $\alpha_{\text{eff}}(\Delta\lambda)$, can be defined for a given window region. For phosphorus smoke these values and the $C \cdot \ell$ range over which they can be reasonably used are shown in Table IV.

REFERENCES

1. G. O. Rubel, An Aerosol Kinetic Model for the Condensational Growth of a Phosphorus Smoke (U), Proceedings of the Smoke/Obscurants Symposium III, Vol. II, Technical Report DRCPM-SMK-T-002-79, APG, MD, pg 729 (1979). CONFIDENTIAL
2. R. H. Frickel, G. O. Rubel, and E. W. Stuebing: Relative Humidity Dependence of the Infrared Extinction by Aerosol Clouds of Phosphoric Acid (U), Proceedings of Smoke/Obscurants Symposium III, Vol. II, Technical Report DRCPM-SMK-T-002-79, APG, MD, pg 517 (1979). CONFIDENTIAL.
3. M. E. Milham, D. H. Anderson, R. H. Frickel, and T. L. Tarnove, New Findings on the Nature of WP/RP Smokes, ARCSL-TR-77067, Chemical Systems Laboratory, APG, MD (1977). ADB-020554.
4. G. O. Rubel, Droplet Growth in a Phosphorus Smoke, CSL Technical Report, APG, MD (1980).
5. Chemical Rubber Company, Handbook of Chemistry and Physics.
6. D. Anderson, Chemical Systems Laboratory, APG, MD. Private Communication.
7. G. C. Lindauer, and A. W. Castleman. Initial Size Distribution of Aerosols, Nucl. Sci and Eng. 43, 212 (1971). E. R. Cohen and E. U. Vaughn, Approximate Solution to the Equations for Aerosol Agglomeration, J. Coll. and Interface Sci. 35, 612 (1971).

*STUEBING, FRICKEL, & RUBEL

8. M. R. Querry and I. L. Tyler, Complex Refractive Indices in the Infrared for H_3PO_4 in Water, J. Opt. Soc. Am. 68, 1404 (1978).

9. O. W. Edwards, R. L. Dunn, and J. D. Hatfield, Refractive Index of Phosphoric Acid Solutions at 25°C, J. of Chem. and Engr. Data 1, 508 (1964).

10. E. W. Stuebing, Deviations from Beer's Law Which Sometimes Prevent Defining a Single Overall Extinction Coefficient for a Smoke in Each Atmospheric Window, Proceedings of the Smoke Symposium II, DRCPM-SMK-T-004-78, Office of the Project Manager for Smoke/Obscurants, Aberdeen Proving Ground, MD (1978).

11. L. A. Riggs, "Light as a Stimulus for Vision", in Vision and Visual Perception, C. H. Graham, ed., John Wiley & Sons, Inc, N.Y., NY (1965).

(307)-308x

**DA
FILM**